

THE ESCALATION CONSEQUENCES OF ACCIDENTAL SHOCK LOADS

Steve Walker and Manjit Klair, SLP Engineering London

ABSTRACT

This paper describes work performed to determine the escalation consequences of accidental shock loads. Shock loads experienced by essential safety systems such as fire water pumps, emergency generators and fire water mains are calculated resulting from ship impact loads, internal and external hydrocarbon explosions.

Two methods are described to calculate the out of balance loads on a North Sea platform due to explosion venting and wall failure. Direct loading from external explosions is also considered.

A simple method of calculation of global platform response is described. General horizontal accelerations of the order of 2m/s^2 (0.2g) were predicted. These accelerations may in turn be amplified at equipment locations by anti-vibration mounts.

Relative displacements between modules have also been found to threaten the integrity of piping associated with safety and process systems.

The general features of the response to these shock loads are described as a case study with reference to the safety case prepared for a major northern North Sea platform.

1. INTRODUCTION

This paper is a description of the work performed by SLP Engineering London for the determination of essential systems integrity under severe vibration and shock loading. The approach described consists of an assessment of the whole platform from the point of view of the ability of essential systems to withstand the effects of severe accident conditions. The accidental conditions considered were more severe and less likely than those used for design. In the case of the internal hydrocarbon explosion the loading involves consideration of the failure of confining walls and calculation of the reaction loads on the main structural framing.

For the ship impact case a time history of global loading on the jacket was calculated. We are not directly concerned with the local deformation of the structure or the energy absorbed by the ship. The global elastic displacement time history of the jacket and topsides was required. A conventional energy approach is not adequate in these circumstances and a load time history was postulated for the applied load from the ship.

A number of major categories of essential systems were identified:-

1. Emergency lighting systems
2. Emergency power supply and battery systems
3. P.A., telecommunication systems and navigation aids
4. Fire water systems
5. Emergency shut down systems
6. Halon systems

The objectives of the work were:-

1. To quantify the peak displacements, accelerations and duration of shock loadings on essential safety systems and equipment items resulting from major accidental events.
2. To identify major piping runs which would be vulnerable to shock loadings from major accidental events through module relative displacements.

The work involved:-

1. Calculation of out of balance loads due to internal and external credible hydrocarbon explosions.
2. Calculation of the global load time history during ship impact.
3. Preparation of a list of critical locations containing essential systems and equipment.
4. Calculation of acceleration and displacement time histories at essential system locations.
5. Calculation of peak relative displacements at the ends of major pipe runs between modules.

The results of the analysis are described with reference to the case study parameters described in the next section.

2. DESCRIPTION OF THE CASE STUDY EXAMPLE

The structure considered is a major eight legged North Sea platform standing in a water depth about 130m. A schematic of the topsides arrangement is shown in Figure 1. The process is located in module M1 next to the wellhead area. Module M2 is the utilities module with the accommodation module M3 at the other end of the platform. This module also serves as the temporary refuge (TR). This accommodation module is mounted on anti-vibration mounts which isolate the module from machinery induced vibrations.

The internal explosion considered was a credible scenario more severe than the design case taken for design of the blast walls between module M1 and M1a and is assumed to initiate on the back wall of level 3 of the process module. Level 3 of the module is completely open on three sides. The overpressure was assumed to be 1.7 bar with a duration of 100 milliseconds. The rise time of the explosion was assumed to be 50 milliseconds.

3. CALCULATION OF LOADS

The two major sources of out of balance loads from explosions are; reaction loads from the expulsion of vented gases and side loads due to the ignition of an external gas cloud which has drifted to one side of the platform. This latter cause was not considered on the basis that the probability of this event was low.

Internal Hydrocarbon explosion

In the Cullen document¹, it was reported that 'a number of witnesses spoke of the severe vibration associated with the initial explosion. People were thrown off chairs and knocked over'. It is consequences of this kind that this work was designed to simulate.

During a vented internal explosion there will be an out of balance lateral force on the module. Consider the situation shown in figure 2 which represents an explosion in an empty module vented through the single vent of area A. The ignition point was located on the back wall and the flame front is shown travelling to the right. The ambient external pressure is P_0 and the instantaneous overpressure is δP . The velocity of the unburnt gases ahead of the flame through the vent is U.

At first sight it seems that the out of balance force on the module will be equal to δPA less any net forces on internal equipment, piping and vent obstructions acting towards the right. In fact the time for pressure disturbances to cross the module may be appreciable and the inertia of the unburnt products and external atmosphere will affect the net force.

The gas velocity of the unburnt products may be estimated from the Rankine-Hugoniot relations² for the change of density and pressure across a shock wave following Catlin et al.³.

$$\text{i.e.} \quad \frac{U}{c} = \frac{\delta P}{P_0} \frac{1}{\gamma} \left\{ 1 + \frac{(\gamma + 1)}{2\gamma} \frac{\delta P}{P_0} \right\}^{-1/2} \quad (1)$$

where U is the unburnt gas mixture velocity in m/s
 γ is the ratio of specific heats for the mixture (taken to be 1.4)
 c is the velocity of sound in the unburnt mixture (taken to be 338 m/s).

The pressures in this equation are in N/m^2 .

This approximation assumes that the unburnt mixture is moving with a velocity corresponding to that behind a weak shock/pressure wave which has passed through the module. The properties of the burnt mixture behind the flame front differ from those given above.

The density of the unburnt mixture ρ may also be related to the overpressure by:-

$$\frac{\rho}{\rho_0} = \left\{ 1 + \frac{(\gamma + 1) \delta P}{2\gamma P_0} \right\} \left\{ 1 + \frac{(\gamma - 1) \delta P}{2\gamma P_0} \right\}^{-1} \quad (2)$$

The net force on the gas volume contained in the module within the contour ABCD may be related to the rate of change of momentum of the enclosed gas. This is equal to the momentum flux of the expelled gas ρU^2 unless U is greater than the local speed of sound at the vent. If this is the case then a second shock wave front is set up at the vent which will restrict the flow. Obstructions at the vent such as louvres may accelerate the flow locally and induce these standing shock waves. The back pressure for confined flow may be represented by a loss factor representing the loss of momentum encountered by the flow⁴.

A 1.7 bar overpressure explosion gives a subsonic peak gas velocity of 262m/s coinciding with the time of peak overpressure. The density at this point is twice the ambient unburnt gas density (1.225 kg/m³). Local supersonic flow occurs at about 2.8 bar overpressure. Figure 3 shows the time history of the flow in terms of the local Mach number defined as the ratio of the gas velocity to the local speed of sound which is 395m/s at the time of peak overpressure. The pulse duration was 100 milliseconds. The mass flux of unburnt gas mixture through the vent was 632 kg/s per square metre of vent area. This corresponds to a peak reaction force of 17 Tonnes for each square metre of vent area.

Figure 4 compares the reaction loads for the case study module calculated by the two methods. The module had a width of 46m and height 9m with a single large vent which spanned the whole module width. The reaction loads calculated from the gas momentum flux are generally below the out of balance load derived from consideration of the overpressure on the back wall but coincide at the peak. The out of balance pressure load is hence a conservative estimate. The peak load is about 7,000 Tonnes in this case. These values assume no gross failure of the back wall of the module.

In the actual case study, the peak pressures given were in excess of the nominal capacities of the walls, floors and ceilings of the area subject to explosions. Even though local failure of floors is possible, the ingress of gas into the level below is not considered to be of sufficient magnitude as to build up a structurally damaging overpressure. No net vertical force was hence applied to the computer model.

As a result of the expected wall failure the out of balance forces were calculated directly from the dynamic reaction forces on the framing of the failed wall.

Where the wall capacity was exceeded, the reaction load on the supporting primary structure was calculated using Biggs' method, reference 5. The wall was idealised as a one degree of freedom system spanning vertically with pinned ends. The time history of the reaction loads was calculated using the SLP in-house computer program NLOSC. This reaction load was calculated per metre of width of the wall and applied to the available nodes in the computer model. The reaction load time history for the framing between modules M1 and M1a is given in figure 5. The static capacity of this wall was calculated to be in the region of 0.65 bar.

The wall was assumed to be breached at the time of maximum deflection at about 200 milliseconds. Any oscillations of the wall following the pressure pulse have been ignored. No load was assumed to act subsequently on the opposite wall of the wellhead area as the pressure had subsided by this time.

Ship Impact

The energy of an internal explosion based on applied force times displacement is in the region of 3.3 MJ compared with ship impact energies of up to 14 MJ (corresponding to a ship of 5000T hitting broadside at a velocity of 2 m/s with an added mass coefficient of 1.4). Of this 14 MJ, 10MJ may be considered to be absorbed by the ship with further energy absorbed by local deformation of the impact zone. This ties in well with the DEN/HSE⁷ requirement of leg absorption capacity of 4MJ. Here we are interested in the residual energy which goes into the movement of the whole structure in an elastic sense.

The DnV background technical note on the subject indicates a peak impact force of 30MN at a displacement of 1m. This is equivalent to an impact energy of the order of 15MJ. Considering the force acting on the ship, and assuming a linearly increasing contact force gives a duration of about 0.5 seconds. The load time history used is shown in Figure 6.

A global time history simulation of the motion of the jacket and ship was performed by SLP using in-house developed software. Assuming the linearly increasing contact force it was shown that the jacket would move away from the ship after the peak contact force was reached. No re-impact with the ship was predicted.

The load was applied at level +5m in the jacket weak direction.

4. DECOMPOSITION OF RESPONSE COMPONENTS

Large computer models are not suitable for dynamic response analysis as the number of modes and frequencies required to give a realistic estimate of response soon becomes unmanageable.

The displacements 'X' and accelerations 'X' of a given point on the structure were considered to consist of a number of components:-

1. The global sway response of the platform at the top of the module support frame (MSF) denoted by 'X_g'.
2. The relative displacements of the module support points resulting from the elastic deformation of the MSF 'X_r'.
3. The motion of the relevant module floor relative to the module support points at the MSF 'X_m'.

The approach consisted of constructing a model which efficiently represented module relative displacements 'X_r' and module floor displacements 'X_m'. The global displacements 'X_g' were obtained using representative springs to model the jacket structure. These springs were included as part of the overall dynamic model. Lumped masses were included to represent the effective jacket mass and added mass at the level at which the springs were attached.

Eight springs were included in the model to represent the stiffness in the transverse direction, four springs were included for the longitudinal direction and a rotational spring was included at the jacket geometric centre to bring the rotational stiffness up to a value consistent with the full platform dynamic jacket analysis. All these springs were attached to a rigid frame at the +5m level.

Calibration was achieved by matching the first three global natural periods in sway and torsion.

Given a natural period T_n, the effective stiffness K_e in this mode is given by:-

$$T_n = 2\pi \sqrt{(M/K_e)} \quad (3)$$

where M is the mass (or moment of inertia) in this mode.

The stiffness calculated in this way gave good results as far as dynamic response was concerned, as the main response parameters (load duration/natural period) were automatically correct.

5. STRUCTURAL MODELLING

As stated above, the jacket below +5m was represented by rotational and linear springs attached to this level.

The module support frame and deck were represented fully in order that deck stiffness and reliable module relative displacements would be derived. The mass distribution in this area as well as the cellar deck was incorporated into the model.

In view of the widespread nature of the P.A. and other systems it was necessary to locate master degrees of freedom where responses were calculated at almost all levels of all modules. Additional master degrees of freedom were located on the MSF, flare boom and derrick in order to isolate local module responses.

The accommodation module, module M3 was supported on four anti-vibration mounts. The stiffnesses of these mounts were modelled by three linear springs in orthogonal directions connected to the MSF horizontal beams at deck level. The AVM stiffness values were supplied by the manufacturer.

Although the AVM's are strongly non-linear in their vertical displacement resistance behaviour, stiffness values could be obtained for the four mounts in the three directions in the region of the curves corresponding to the dead loads present in-place. The AVM horizontal stiffness behaviour was found to be linear at small displacements.

A modal analysis was performed after assembly of the structural computer model. This analysis gives the natural modes of vibration of the structure and is an essential precursor to the dynamic response analysis as the response is built up as a combination of the mode shapes derived in this way. In all 250 master degrees of freedom were defined and 50 mode shapes were calculated.

The typical duration of the blast load of 0.2 seconds was within the resolution of the modal superposition method and SLP was satisfied that enough modes had been obtained.

Examination of the mode shapes revealed that module M1 was particularly vulnerable to excitation at periods of around 0.8 seconds due to the presence of the AVM's. Global motion of the jacket was expected at around 3 seconds period.

A damping value of 2% of critical was associated with the first three global modes as recommended by DnV⁶ to include the induced hydrodynamic damping. All other modes were allocated a damping of 0.1% which is recommended for welded structural steel in air. The modes associated with response of module M1 on the AVM's had a damping value of 10% of critical as recommended by the AVM manufacturer.

The simplified computer model of the total topsides and platform was loaded dynamically and module floor displacements and accelerations derived directly.

6. RESPONSE RESULTS

Figures 7a to 7c show the response of the platform to an explosion on level 3 of module M1 at various times after the explosion. In Figure 7a at 0.1 seconds, module M1 is beginning to deform. In Figure 7b at 0.5 seconds the energy has been transmitted into the module support frame (MSF) and the whole platform has begun to move in the direction of the blast loading. Figure 7c at 1 second shows module M1 rebounding and modules M2 and M3 near their peak response.

Two major components of response shown in Figure 8 are evident. The first is the global response of the jacket at a period of about 3 seconds corresponding to global sway of the jacket. Superimposed on this is a response due to the motion of module 3 on its anti-vibration mounts at a period of about 0.3 seconds. Some torsion of module M3 is also indicated at later times (after 1 second) as the effect of the explosion propagates through the structure after the load has been dissipated. At these later times displacements perpendicular to the direction of the blast build up due to dynamically induced moments resulting from off-centre centres of gravity.

Acceleration levels in other modules were found to be less severe.

The internal explosion results in peak accelerations of the order of 0.2 times the acceleration due to gravity on level 1 of module M3, where most of the essential systems are located.

The Ship Impact load case gives accelerations of the order of 0.2g generally throughout the platform. Vertical accelerations of about 0.5m/s^2 are present at MSF level. The AVM's on M3 have the effect of amplifying these vertical accelerations.

The acceleration time history for the same node and load case is given in figure 9. This shows that the acceleration passes through two groups of peaks during the three second simulation. The absolute peak occurs in the second group which would more likely be of lower amplitude than the first due to the high damping of the AVM's. For this reason the recommended maximum value of 3.5 m/s^2 is considered more typical.

Finally from the relative displacements at the ends of major pipe runs between modules, only one location was found to be relevant from the point of view of essential systems and this was the fire water main running between level 1 of module M3 and module M2. A maximum relative displacement of 20mm is calculated for these two nodes.

The other connections between M1, M2 and M3 were already designed to accommodate relative displacements of these magnitudes without high loads being generated.

7. CONCLUSIONS

1. For the explosion load cases, global platform displacements of up to 45mm are predicted with associated peak accelerations of up to 2m/s^2 at MSF level. The presence of anti-vibration mounts on the accommodation module M3 gives rise to an amplification of acceleration associated with rocking of M3 on its mounts at about 0.3 seconds natural period giving rise to high accelerations on level 1. This level is associated with the fire water pumps.
2. The relatively new platform design examined in this study stood up well to the imposed loads as modules were free to move relative to each other. Older platforms with small modules kept in place under their own weight may not fare so well. We would recommend that shock effects are considered in any future safety case.

REFERENCES

1. Cullen, 'The Public Enquiry into the Piper Alpha Disaster', HMSO, London, 1990.
2. Massey B.S., 'Mechanics of Fluids', Van Nostrand Reinhold Company, 3rd Edn., 1975.
3. Catlin C.A., Mihsein M. and Younger B., 'The Blast Loading Imparted to a Cylinder by Venting of a Confined Explosion', Proc. 2nd Intl. Conference and Exhibition, Offshore Structural Design Against Extreme Loads, ERA Technology., London, November 1993.
4. Hoerner S.F., 'Fluid Dynamic Drag', Hoerner Fluid Dynamics, 1965.
5. J.M. Biggs, 'Introduction to Structural Dynamics', 1964, McGraw Hill.
6. 'Rules for the Design, Construction and Inspection of Offshore Structures', Appendix G, 'Dynamic Analysis', DnV 1977.
7. 'Guidance on the Design and Construction of Offshore Installations', 4th edn., HMSO, DEN/HSE, 1990.

Figure 1	Schematic of Topsides Arrangement
Figure 2	Vented Internal Explosion
Figure 3	Gas Velocities and Overpressure
Figure 4	Reaction Loads on Module
Figure 5	Load Time History from Failing Blast Wall
Figure 6	Ship Impact Prescribed Contact Force
Figure 7	Platform Response
Figure 8	Displacement Level 1 Accommodation Module
Figure 9	Acceleration Time History

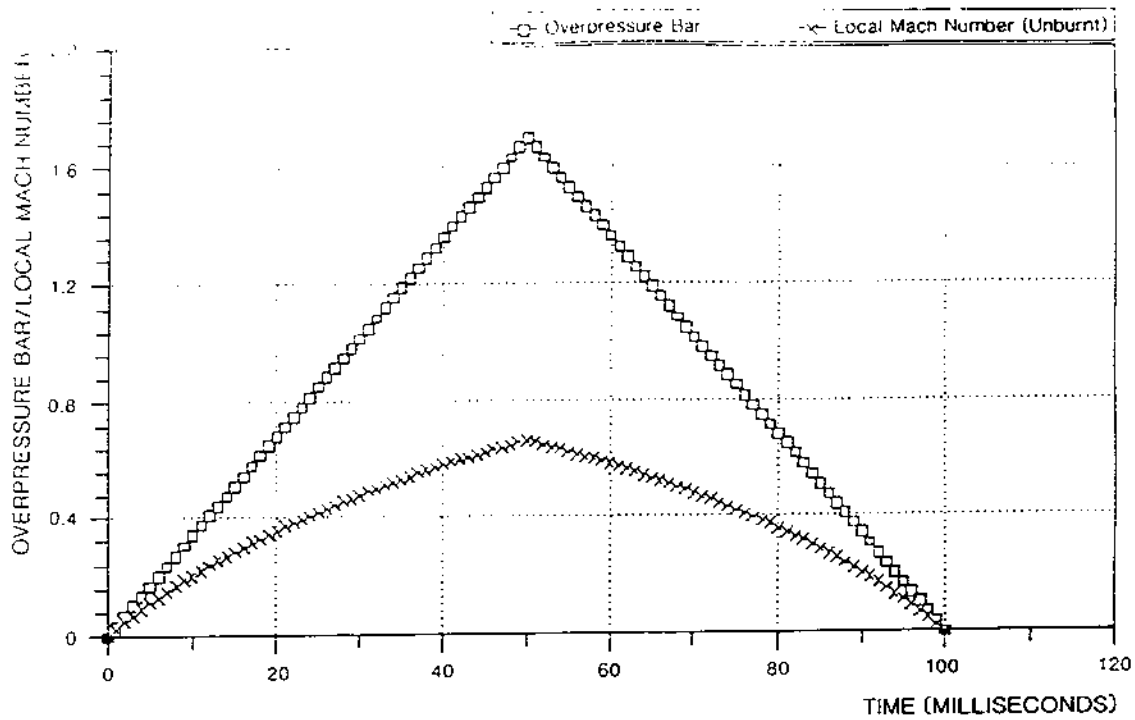


FIGURE 3

REACTION LOADS ON MODULE

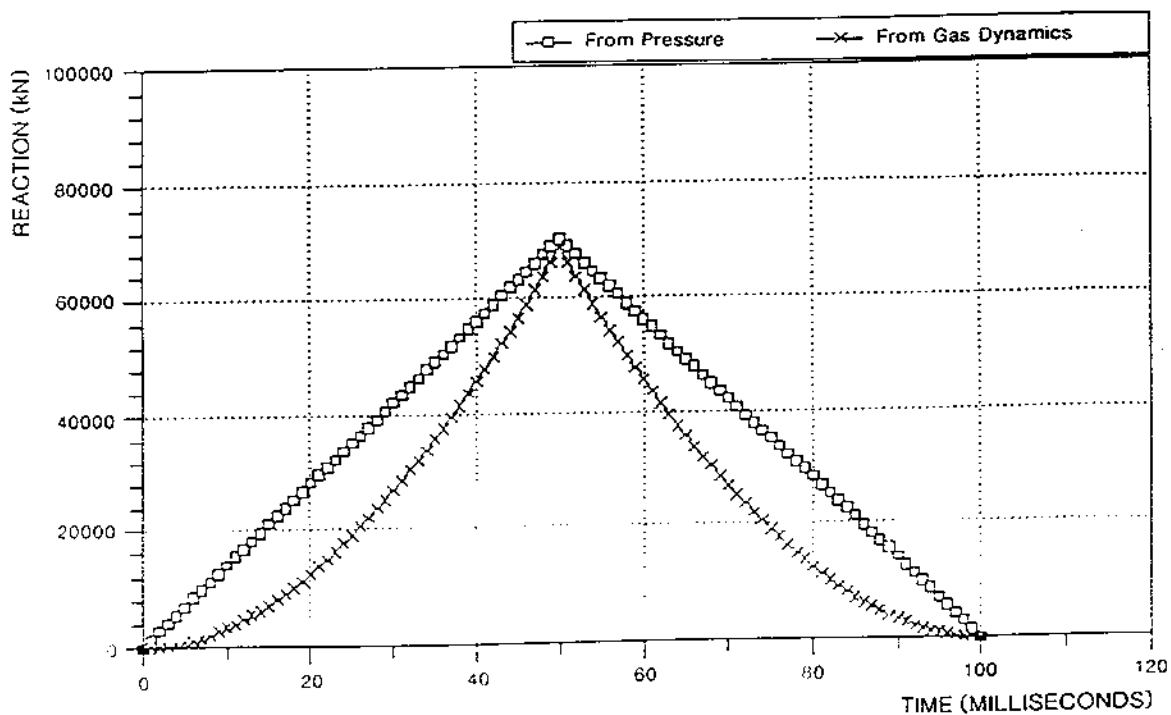


FIGURE 4

GAS VELOCITIES AND OVERPRESSURE

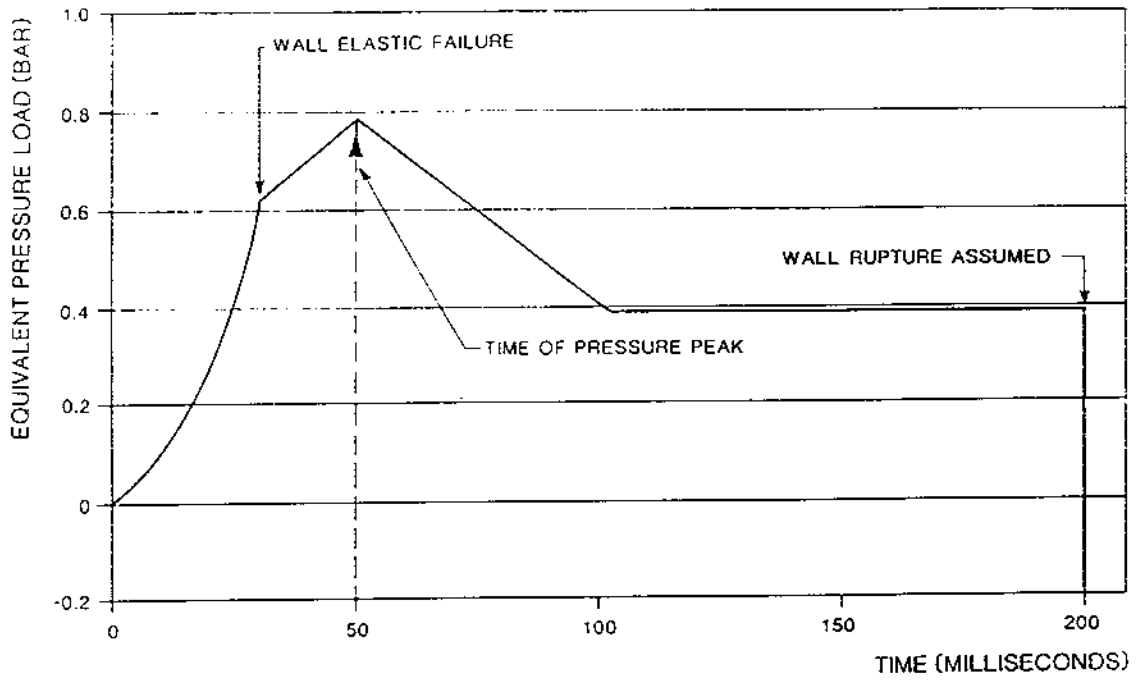


FIGURE 5

LOAD TIME HISTORY FROM FAILING BLAST WALL

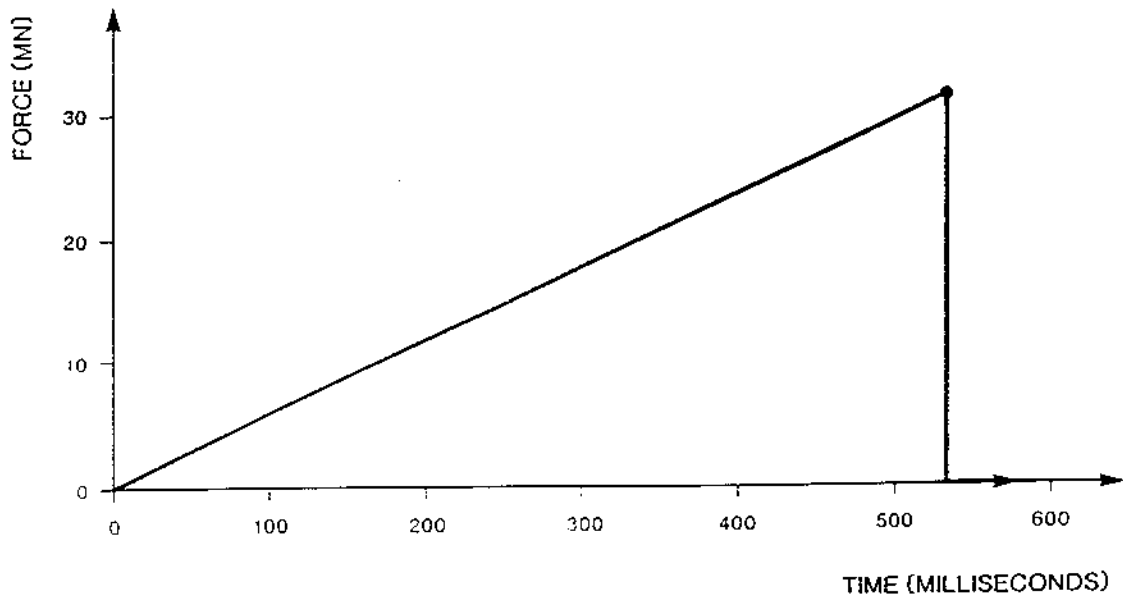


FIGURE 6

SHIP IMPACT PRESCRIBED CONTACT FORCE

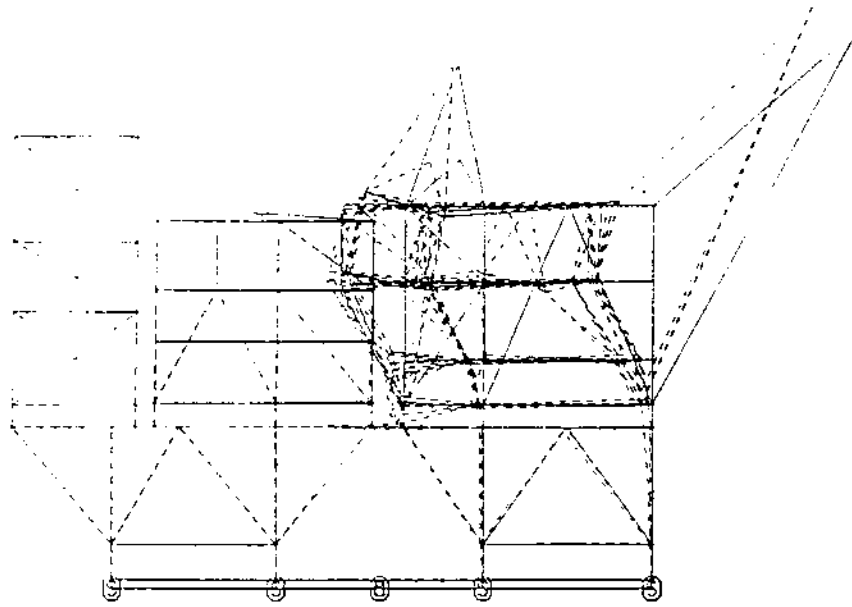


FIGURE 7a PLATFORM RESPONSE AT TIME 0.1 SECONDS

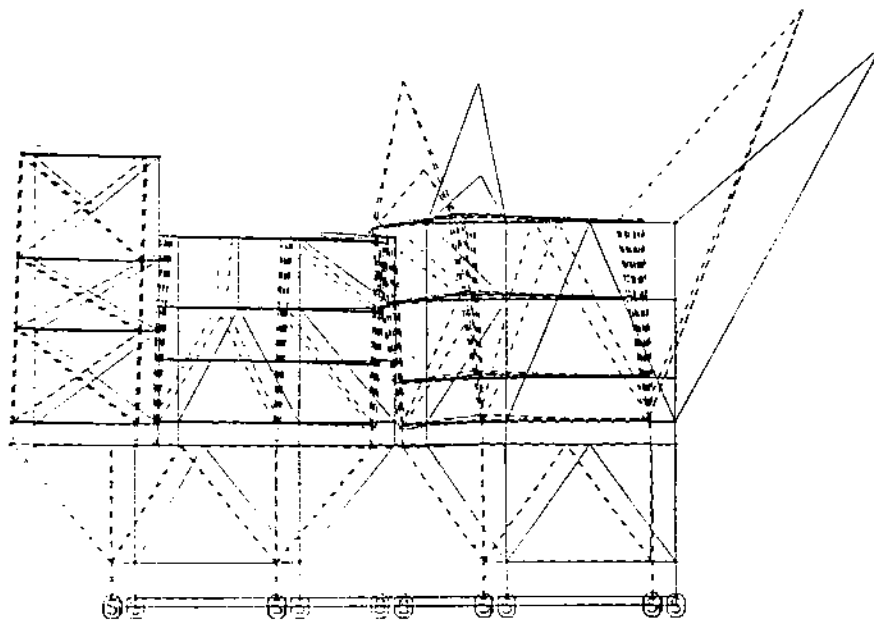


FIGURE 7b PLATFORM RESPONSE AT TIME 0.5 SECONDS

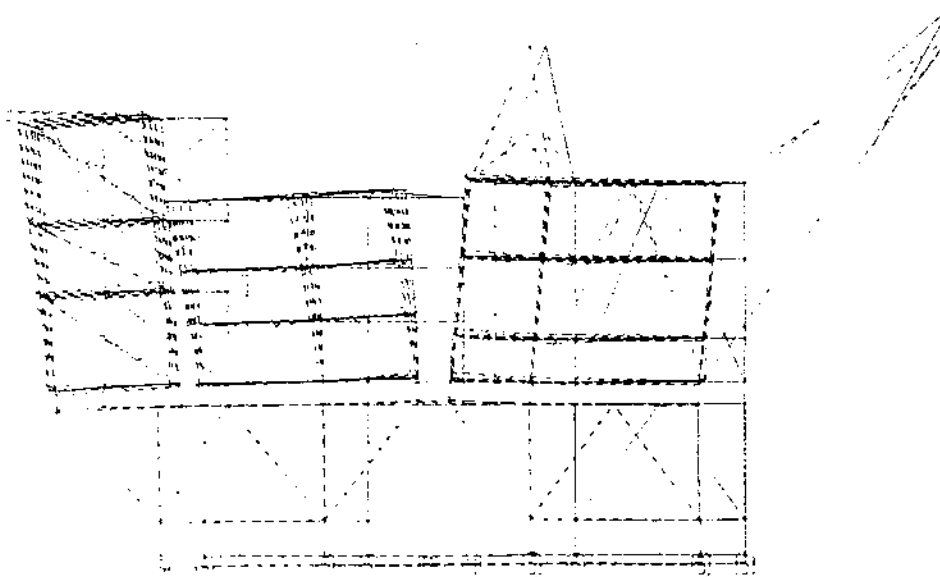


FIGURE 7c PLATFORM RESPONSE AT TIME 1.0 SECONDS

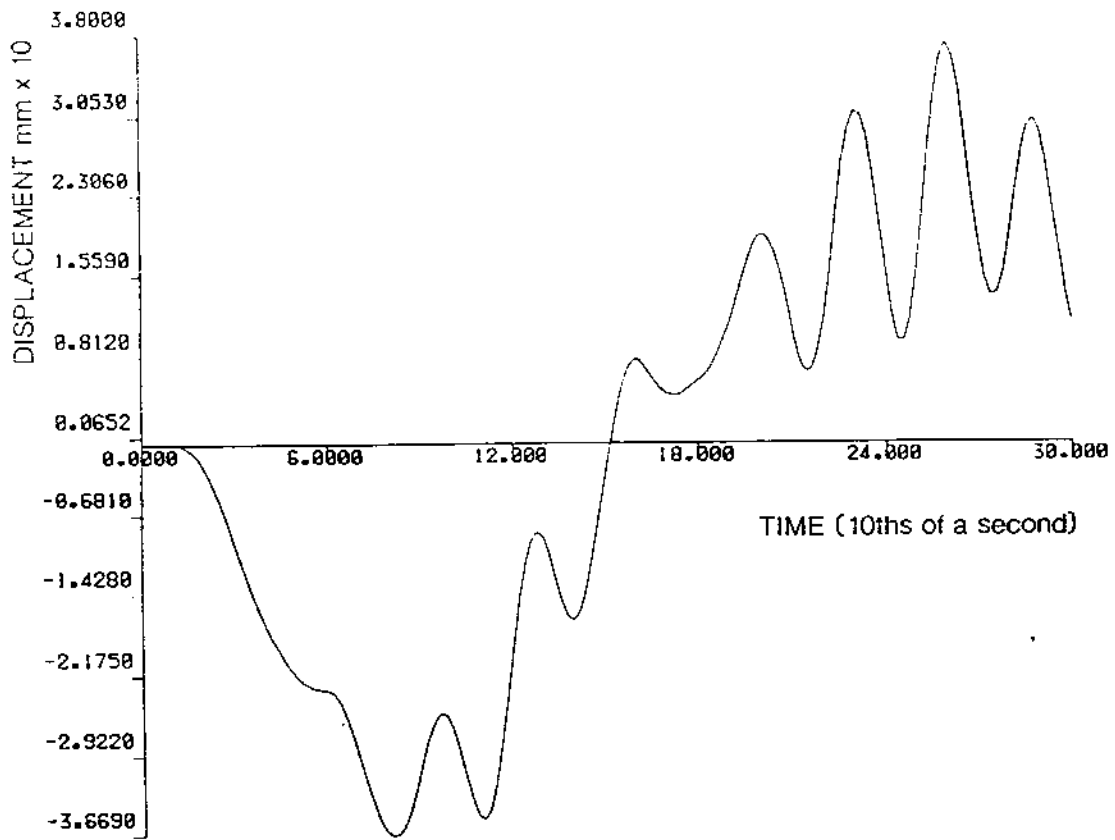


FIGURE 8

DISPLACEMENT LEVEL 1 ACCOMMODATION MODULE

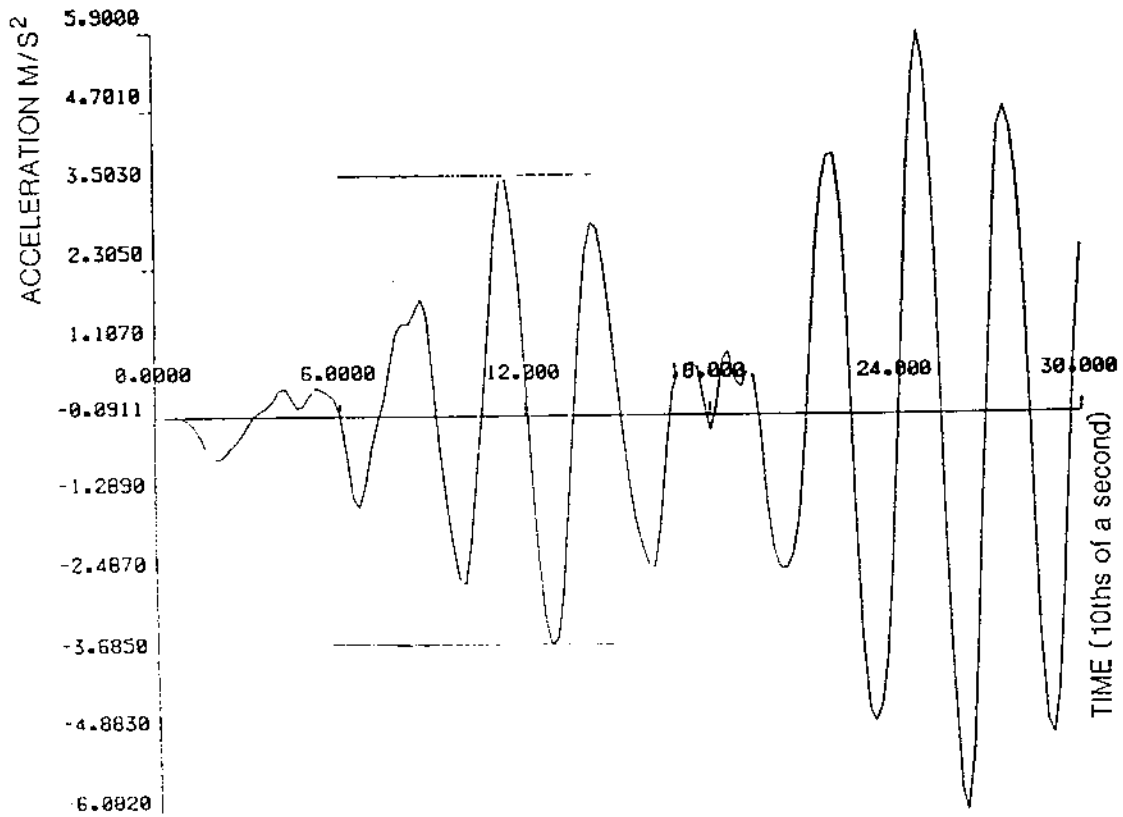


FIGURE 9

ACCELERATION TIME HISTORY